



## **Primary filtration of municipal wastewater with sludge fermentation – Impacts on biological nutrient removal**

Downloaded from: <https://research.chalmers.se>, 2025-12-04 23:38 UTC

Citation for the original published paper (version of record):

Ossiansson, E., Bengtsson, S., Persson, F. et al (2023). Primary filtration of municipal wastewater with sludge fermentation – Impacts on biological nutrient removal. *Science of the Total Environment*, 902. <http://dx.doi.org/10.1016/j.scitotenv.2023.166483>

N.B. When citing this work, cite the original published paper.



could be reduced by 11–18 %. The estimated total biogas production was similar for pre-treatment with primary settler and RBF with fermentation. RBF without fermentation gave the most favourable energy balance, but did not reach the same low effluent value for total nitrogen as RBF with fermentation.

## 1. Introduction

Stricter effluent requirements for municipal wastewater treatment plants (WWTPs) are implemented to lower the environmental impact in the receiving waters. The key to lower effluent values of nitrogen in conventional municipal wastewater treatment is well known: full nitrification, and sufficient carbon source and anoxic retention time to reach low concentrations of nitrate and nitrite through denitrification. Extensive carbon removal in wastewater pre-treatment is beneficial for the energy balance (Arnell et al., 2017; Behera et al., 2018; Siegrist et al., 2008), but on the other hand, it can be detrimental for the biological nutrient removal (BNR) if the wastewater C:N ratio becomes too low. Addition of external carbon source as a means to enhance BNR is associated with heavy environmental burden (Gustavsson and Tumlin, 2013; Remy et al., 2014).

Filtration of influent wastewater as primary treatment has been applied with several types of filters, such as drum-, disc-, and rotating belt filters (RBFs; Caliskaner et al., 2021). Advantages of primary filtration compared to primary settling are reduced footprint (Franchi and Santoro, 2015) and the possibility to control and enhance particle separation (Rusten et al., 2017). Primary settlers typically have total suspended solids (TSS) reductions of 50–55 % (Amerlinck, 2015; Patziger and Kiss, 2015). Research on drum- and disc filters resulted in average TSS removal of 66/46/43 % with mesh sizes of 30/40/100  $\mu\text{m}$  without extensive cake filtration and no chemical addition (Väänänen et al., 2016). Addition of 2–4 g/L cationic polymer increased the TSS reduction to 80–90 %. Polymer addition prior to filtration has been successful also for RBF filters, resulting in an increase in COD removal from 23 to 47 % after addition of 2 g polymer/ $\text{m}^3$  (Franchi and Santoro, 2015). As a comparison, COD removal in primary settling with 2 h retention time has been reported in the range of 26–40 % (Tas et al., 2009). In previous studies, primary filtration has predominantly been studied without addition of chemicals. Information about the particle size distribution, and its impact on COD removal in the filter enables a better removal prediction for wastewaters with different characteristics. An empirical model for prediction of TSS removal in an RBF based on influent TSS has been proposed (Behera et al., 2018), as well as more complex dynamic models (Boiocchi et al., 2020; Khan et al., 2021).

In recent years, filter primary sludge (FPS) has rendered interest as a potential substrate for sustainable internal carbon source production (Christensen et al., 2022; Da Ros et al., 2020; Ossiansson et al., 2023). The volatile fatty acids (VFAs), which are produced in the fermentation of FPS, can be separated from the sludge by e.g. centrifugation (Andreassen et al., 1997). This can, however, be difficult due to increased concentrations of humic acids and phosphate, decreased particle sizes, and altered surface charges (Liu et al., 2021). A part of the soluble COD will not end up in the fermentate, but in the solid fraction. As a consequence, if the fermented sludge has a total solids (TS) content of 3 % and is dewatered to 10 %, about 30 % of the produced carbon source cannot be directed to the biological treatment. This loss of carbon source has been reflected in full-scale scenarios for VFA production at WWTPs, where a considerable fraction of the produced VFA was left in the solid fraction after dewatering of the fermented sludge (Bahreini et al., 2021; Canziani et al., 1996; Christensen et al., 2022). Therefore, it is desirable to find a novel method for the transfer of VFAs from sludge to wastewater, without loss of valuable carbon source.

Pre-treatment with filtration has pronounced effects on the subsequent BNR at WWTPs. The aeration energy requirements for BNR have decreased by 30–50 % in various reactor systems with filtration pre-treatment compared with without pre-treatment (Franchi and Santoro,

2015; Pasini et al., 2021; Razafimanantsoa et al., 2014; Rusten et al., 2016). Since much of the bioavailable organic carbon in the wastewater passes through the filter, nitrogen removal in BNR with or without filtration can be similar, and filtration can even result in higher denitrification rates (Razafimanantsoa et al., 2019). When comparing filtration with sedimentation in primary settlers, higher removal of particles in the 5–45  $\mu\text{m}$  range with filtration can decrease the volume requirement for BNR by as much as 40 % (van Nieuwenhuijzen et al., 2004). But if the organic carbon removal is extensive in the filtration step, the nitrogen removal can decrease with filtration compared with settling, as indicated by simulations (Behera et al., 2018). Fermentation coupled with filtration may well impact design and operation of the subsequent BNR, since the amount of bioavailable carbon is expected to increase by the fermentation. An improvement in nitrogen removal with fermentate addition from filter sludge has been shown in lab-scale (Bahreini et al., 2021). However, it is yet uncertain how filtration coupled with fermentation would affect e.g. aeration- and volume requirements, effluent values and the resulting energy balance.

In this study, we propose and assess a novel pre-treatment for wastewater: chemically enhanced RBF filtration in combination with carbon source production from FPS through fermentation at ambient temperature. This process was evaluated from pilot-scale testing at Källby municipal WWTP in Lund (Sweden). The removal of suspended matter by the filter and the potential effects on the subsequent BNR, as well as the energy performance were investigated. Empirical models for reduction of TSS and COD in the filter were tested to provide a simple tool for prediction of removal efficiency. A strategy of recycling the fermented sludge to the wastewater, with separation of particles through filtration was evaluated as a means to utilize nearly all of the produced VFAs for enhanced biological phosphorus removal (EBPR) and/or denitrification. Furthermore, we used the Benchmark Simulation Model no. 1 (BSM1) and calculation of required BNR volumes to compare primary settler, RBF, and RBF with fermentation as pre-treatments with respect to volume requirement in BNR and effluent values, as well as electricity demand and biogas production. Thereby, the pre-treatments' impact on BNR is highlighted from several aspects.

## 2. Material and methods

### 2.1. Pilot plant operation and sampling

The influent wastewater flow rate to the pilot plant was proportional to the Källby WWTP flow rate, with an average of 12  $\text{m}^3/\text{h}$ . Limits of minimum 6–8  $\text{m}^3/\text{h}$  and maximum of 18–20  $\text{m}^3/\text{h}$  were set to the pilot plant. With this flow variation, the hydraulic load and TSS load were representative to the full-scale plant, allowing for more realistic conditions for filtration compared to a case with fixed flow rates. The RBF (SF1000, Salsnes Filter) was subjected to an average load on submerged filter area of  $47 \pm 11 \text{ m}^3/(\text{m}^2, \text{h})$  during the first year of operation July 2020 to July 2021. When the filter was operated again from November 2021, the plant was first run for a few weeks to stabilise. Then fermented sludge was recirculated back to the wastewater (after the influent sampling point, Fig. S1). During the period with recirculation December 2021 to May 2022, the load was  $45 \pm 16 \text{ m}^3/(\text{m}^2, \text{h})$ . With this operating mode, the TSS load to the filter was increased during peak-loads which occurred every 1–2 h when the fermentation reactors effluent pumps were running. The filter level was set to 200–230 mm.

A cationic polymer (Superfloc 6260, Kemira Kemi) was dosed based on a set value of 1–1.5 g/ $\text{m}^3$ , with addition of 2–3 g/kg TSS. Online measurement of TSS with VisoLid (WTW) was used to control the

polymer dose. The polymer was chosen based on jar tests with polymers of different ionic strength and chain length. Anionic polymer gave a high separation in lab-scale, but the flocs were too weak to be separated in the pilot plant filter. Two tanks in series, with an average total retention time (RT) of  $9 \pm 3$  min, were used for flocculation with mixing at 70 and 50 rpm respectively. Wastewater was collected as 24 h flow proportional composite samples 2–3 days/week and analysed the same day.

Fermentation of FPS was operated at 5 d RT, and ambient temperature. Further details on the fermentation process is available from Ossiansson et al. (2023).

## 2.2. Chemical analyses

VFAs and total alkalinity in the wastewater and in the sludge were measured as acetic acid equivalents (HAc-eq) with 5-point titration according to Ibrahim et al. (2014). Specific VFAs in the fermented sludge were measured with gas chromatography (GC) or high-performance liquid chromatography (HPLC) according to Ossiansson et al. (2023) and converted into COD units. Total nitrogen was analysed by oxidation and chemiluminescence (Shimadzu TOC-L & TNM-L with ASI-L).

Coarse filtration of particles  $>20 \mu\text{m}$  was conducted with paper filters (Munktell No: 110 116). Samples for analysis of ammonium nitrogen and TSS were filtered through  $1.6 \mu\text{m}$  glass fiber filters (Whatman, GF/A No 1820-055). Filters for TSS analysis were dried for 2 h at  $105^\circ\text{C}$ . Cuvettes (LCK 304, Hach) were used for ammonium-nitrogen analysis. Total phosphorus was analysed after acidification with 4 M  $\text{H}_2\text{SO}_4$  with spectrophotometry (Lambda 35, PerkinElmer).

For COD characterisation, 24 h flow proportional samples of both influent and pre-filtered wastewater from the pilot plant were collected. The wastewater was filtered through cloths of 100, 60, 40 and  $10 \mu\text{m}$  pore size (Monofilament twill polyester cloth). For the fine filters of  $5 \mu\text{m}$  (Cellulose nitrate filter, Whatman),  $1.6 \mu\text{m}$  (Whatman, No 1820-055),  $0.45$  and  $0.1 \mu\text{m}$  (Cellulose nitrate filters, Whatman), vacuum suction was applied. A minimum volume of 30 mL wastewater was filtered for all pore sizes. Cuvettes (LCK 114, Hach) were used for all COD analyses.

## 2.3. Calculations

Statistical significance was tested with paired student *t*-test in Excel 2019 (Microsoft). The reductions of TSS and COD (mg/L) in the filter were fitted to linear functions versus the influent TSS concentration ( $\text{TSS}_{\text{in}}$ ) in Origin (OriginLab). Likewise, the TSS reduction (%) was fitted in Origin, using Levenberg Marquardt iteration for the variables  $k_1$  and  $k_2$  in the exponential model in Eq. (1) according to (Behera et al., 2018).

$$\text{TSS}_{\text{red}}(\%) = 100 * (1 - k_1 e^{-k_2 x}) \quad (1)$$

The temperature dependency for VFA concentration in wastewater and the VFA concentration increase were fitted to Eq. (2), since the concentrations were assumed to be representative to the formation rates given the constant RT and reactor solids concentration (Rieger et al., 2013).

$$\text{VFA} = \text{VFA}_{20} \cdot \theta^{(T-20^\circ\text{C})} \quad (2)$$

The increase in VFA concentration in the wastewater ( $\text{VFA}_{\text{Increase}}$ ) owing to addition of the fermented FPS flow ( $Q_F$ ) with VFA concentration ( $\text{VFA}_F$ ) to the wastewater flow ( $Q_{\text{ww}}$ ) was calculated assuming that all the FPS would be recirculated to the wastewater from the fermentation reactor with RT 5 d, thus reaching the full VFA potential. The resulting concentration increase in the wastewater for VFA, phosphate phosphorus and ammonium nitrogen were calculated as for the example of VFA in Eq. (3). Since wastewater and sludge sampling were not always carried out the same day, and RT for the fermentation reactor was 5 d during the first year, the calculation of ratios between COD and nutrients with addition of fermentate were calculated from the mean values of fermentate concentration during a period of  $\pm 4$  d from the

sampling day for wastewater. For the calculation of COD to nutrient ratios, the suspended matter in the fermentate was assumed to be removed before addition to the wastewater.

$$\text{VFA}_{\text{Increase}} = \frac{\text{VFA}_F \cdot Q_F}{Q_{\text{ww}}} \quad (3)$$

## 2.4. Simulations

The BSM1 model, representing a typical activated sludge WWTP for nitrogen removal (Gernaey et al., 2015) was implemented in WEST (DHI). Three pre-treatment alternatives were compared by preparing three corresponding influent matrices (Fig. 1): 1) settler 2) RBF and 3) RBF with fermentation and addition of fermentate solubles to the wastewater (RBFF). All parameter values for e.g. kinetics and electricity usage, as well as stoichiometry were according to Gernaey et al. (2015), and the corresponding influent file (Jeppsson, 2009) was used as basis for the influent matrices.

The influent composition after primary settling was set to the standard values for BSM1, since the primary settler effluent in the benchmark simulation model no. 2 (BSM2) results in similar effluent composition as the influent to BSM1 (Gernaey et al., 2009). Thus, the original influent to BSM1 is regarded as representative for a primary settler effluent after 50 % TSS removal. Based on these considerations, the influent particulate COD for RBF and RBFF ( $X_S^{\text{RBF,RBFF}}$ ), were calculated from the BSM1 influent particulate COD ( $X_S$ ) with Eq. (4). The particle removal in Eq. (4) was calculated from the influent concentration with a linear model (Section 3.3) and subtracted. The raw influent wastewater composition was also calculated, by doubling the particulate fractions ( $X_{S,I,BH}$ ).

$$X_S^{\text{RBF,RBFF}} = 2 \cdot X_S - (a + (b \cdot 2 \cdot X_S)) \quad (4)$$

The inert particulate COD ( $X_I^{\text{RBF,RBFF}}$ ), for RBF and RBFF, as well as particulate nitrogen ( $X_{\text{ND}}^{\text{RBF,RBFF}}$ ) and heterotrophic biomass ( $X_{\text{BH}}^{\text{RBF,RBFF}}$ ) were calculated from the BSM1 influent values of inert particulate COD ( $X_I$ ), particulate nitrogen ( $X_{\text{ND}}$ ), heterotrophic biomass ( $X_{\text{BH}}$ ) and the ratio between  $X_S$  and  $X_S^{\text{RBF,RBFF}}$  as shown in Eqs. (5), (6) and (7).

$$X_I^{\text{RBF,RBFF}} = X_I \cdot \frac{X_S^{\text{RBF,RBFF}}}{X_S} \quad (5)$$

$$X_{\text{ND}}^{\text{RBF,RBFF}} = X_{\text{ND}} \cdot \frac{X_S^{\text{RBF,RBFF}}}{X_S} \quad (6)$$

$$X_{\text{BH}}^{\text{RBF,RBFF}} = X_{\text{BH}} \cdot \frac{X_S^{\text{RBF,RBFF}}}{X_S} \quad (7)$$

The ammonium nitrogen concentration with RBFF ( $S_{\text{NH}}^{\text{RBFF}}$ ) was calculated according to Eq. (8) with the increase from the fermented particulate nitrogen ( $X_{\text{ND}}$ ) and nitrogen in fermented active heterotrophic biomass ( $0.08 \cdot X_{\text{BH}}$ , Eq. (3)), which is solubilised and recirculated to the wastewater. The removal of  $X_{\text{ND}}$  in the standard BSM1 wastewater during settling was set to 20 %, thus a factor of 1.2 is utilised for the influent  $X_{\text{ND}}$  in (8). Likewise, the soluble COD concentration with RBFF ( $S_S^{\text{RBFF}}$ ), was calculated with an increase of soluble COD from fermentation (9). The solubilisations of COD and nitrogen were set as the mean values based on the first year of operation at pilot-scale,  $N_{\text{sol, fermentation}} = 0.33$ , and  $S_{\text{sol, fermentation}} = 0.16$ , which corresponded to an SCOD yield of 163 g COD per g influent volatile solids ( $\text{VS}_{\text{in}}$ ).

$$S_{\text{NH}}^{\text{RBFF}} = S_{\text{NH}} + \text{mean}(1.2 \cdot X_{\text{ND}} - X_{\text{ND}}^{\text{RBFF}} + 0.08 \cdot (2 \cdot X_{\text{BH}} - X_{\text{BH}}^{\text{RBFF}})) \cdot N_{\text{sol, fermentation}} \quad (8)$$

$$S_S^{\text{RBFF}} = S_S + \text{mean}(2 \cdot X_S - X_S^{\text{RBFF}}) \cdot S_{\text{sol, fermentation}} \quad (9)$$

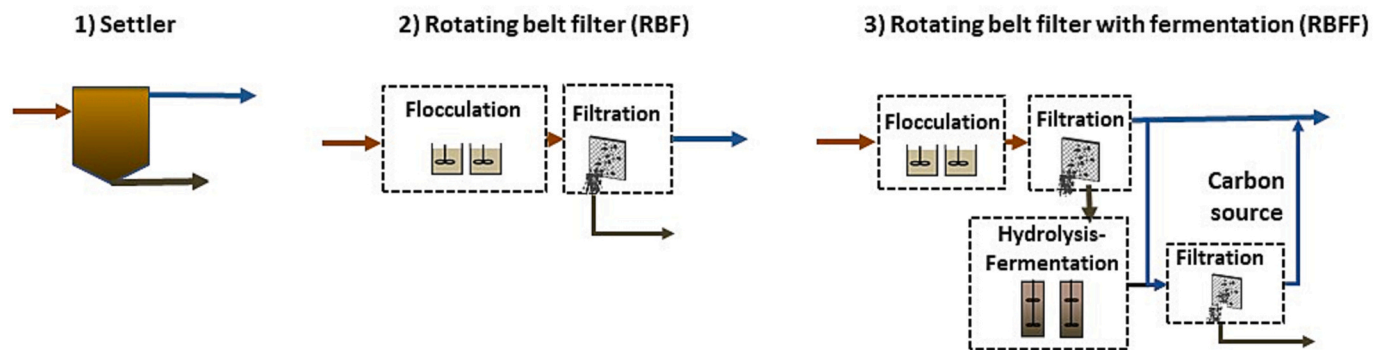


Fig. 1. Wastewater pre-treatments which were compared by simulations.

These calculations resulted in the influent matrices with RBF and RBFF for steady state and dynamic simulations (Table S1). The increase in ammonium nitrogen due to addition of fermentate was on average 2 mg N/L. The RBFF influent contained 107 mg soluble COD/L, compared to 70 mg/L with settler/RBF.

The TSS concentration in the last aerated zone was controlled by a PI-controller for the waste activated sludge (WAS) flow rate to reach 3267 mg TSS/L, the steady state value for BSM1 with standard influent (Gernaey et al., 2015). The allowed WAS flow was set to 30–1000 m<sup>3</sup>/d,  $K_p = -0.5$  and  $K_I = 0.1$  d. The initial value was set to 385 m<sup>3</sup>/d, same as the non-variable WAS-flow in BSM1.

The models were first simulated during 200 d to reach steady state, before 14 d dynamic simulations were initiated. Results with 15 min resolution were used to calculate flow proportional means for the 14-d period of dynamic simulations. Additionally, the effluent values were calculated according to the fractionation proposed in Gernaey et al. (2015). The temperature was set to 15 °C for all simulations.

## 2.5. Calculation of required BNR volumes

The design volumes for simulations of activated sludge were calculated from the German standard procedure (DWA, 2016) to obtain reasonable volumes for the BNR after pre-treatment with settler, RBF, and RBFF with parameters found in Table S2. The influent concentrations used as design basis were calculated from the flow proportional means of the BSM1 influent matrices, where the readily degradable COD in the influent ( $COD_{deg, IAT}$ ) was set to  $S_S$  in the BSM1 influent. The resulting design solids retention times (SRT) was 11.7 d, based on the influent composition in Table S3.

## 2.6. COD and energy balance

For calculation of biogas potential, the VS from primary settler was set to 85 % of TS, and 87 % for filter sludge (Ossiansson et al., 2023). The biomethane potentials were set to 0.32 Nm<sup>3</sup>/kg VS for RBF sludge, 0.27 Nm<sup>3</sup>/kg VS for RBFF and 0.29 Nm<sup>3</sup>/kg VS for settler primary sludge, based on full-scale data and methane potential tests (Blom, 2022). These values correspond well to previously reported measurements (Paulsrud et al., 2014). For WAS, the VS was set to 75 % of TS and the biomethane potential was set to 0.20 Nm<sup>3</sup>/kg VS. The electricity usage for the settler was set to 0.004 kWh/m<sup>3</sup> (Longo et al., 2016). RBF and RBFF electricity usages were set to 0.02 kWh/m<sup>3</sup>, which represents a large filter (Salsnes Filter, 2016), with a reduced capacity of 30 % due to the polymer addition.

## 3. Results

### 3.1. Removal of organics and nutrients in the filter

Overall, the operation of the RBF was stable without any operational problems affecting the process performance. Since both the inflow and TSS concentrations varied, the daily mean TSS load on the submerged filter area was variable, ranging from 3 to 20 kg TSS/ (m<sup>2</sup>, h) with a mean of  $12 \pm 3$  kg TSS/ (m<sup>2</sup>, h). The influent TSS was variable,  $242 \pm 60$  mg/L, whereas the effluent TSS remained rather stable at  $84 \pm 20$  mg/L (Table 1). Reductions of TSS, COD, nitrogen and phosphorus in composite samples were  $64 \pm 10$  %,  $44 \pm 9$  %,  $8.5 \pm 7.8$  % and  $18 \pm 8$  % respectively (Table 1). Polymer addition was  $3.2 \pm 1.0$  g/m<sup>3</sup>, corresponding to  $15 \pm 10$  g/kg TSS. The filter level did not affect the TSS reduction in the range of 200–230 mm during this study (data not shown).

Table 1

Chemical parameters for influent and filtered wastewater, as well as reductions of these during the first year of operation presented as mean  $\pm$  standard deviation. *P*-values for pairwise student *t*-test are also shown.

Parameter	Unit	No. of samples	Influent wastewater	Filtered wastewater	P-value
Total suspended solids	mg/L	102	242 $\pm$ 60	84 $\pm$ 20	<0.001
Volatile suspended solids	mg/L	102	224 $\pm$ 56	79 $\pm$ 19	<0.001
Chemical oxygen demand	mg COD/L	102	528 $\pm$ 110	290 $\pm$ 52	<0.001
Chemical oxygen demand, coarse filtered (20 $\mu$ m)	mg COD/L	99	225 $\pm$ 42	207 $\pm$ 39	<0.001
Chemical oxygen demand, filtered (1.6 $\mu$ m)	mg COD/L	30	146 $\pm$ 29	140 $\pm$ 26	0.253
Ammonium nitrogen	mg/L	102	39.0 $\pm$ 7.1	38.5 $\pm$ 7.7	0.345
Total nitrogen	mg/kg TS	103	55.7 $\pm$ 9.6	50.8 $\pm$ 8.9	<0.001
Total phosphorus	mg/L	102	6.7 $\pm$ 1.3	5.4 $\pm$ 1.0	<0.001
Volatile fatty acids	mg HAC-eq/L	77	23.8 $\pm$ 15.8	20.1 $\pm$ 10.0	0.003
COD to ammonium ratio	g COD/g NH <sub>4</sub> <sup>+</sup> -N	100	13.7 $\pm$ 2.2	7.7 $\pm$ 2.0	0.000
TSS reduction	% of TSS	102		64 $\pm$ 10	
COD reduction	% of COD	101		44 $\pm$ 9	
Nitrogen reduction	% of N	102		8.5 $\pm$ 7.8	
Phosphorus reduction	% of P	101		18 $\pm$ 8	



There was no statistically significant difference in ammonium concentration in influent wastewater compared to filtered wastewater, but a minor difference in VFA concentration could be observed ( $P = 0.003$ ), as the mean value decreased from 23.8 to 20.1 mg HAC-eq/L (Table 1).

### 3.2. COD characterisation

COD characterisation showed that particles  $>10\ \mu\text{m}$  were efficiently removed in the filter with an average removal of 87 %, while the COD in smaller particles passed through the filter (Fig. 2). The average total COD removal in the RBF filtration for the characterised samples was 48 %, whereas the average removal of COD for particles larger than  $100\ \mu\text{m}$  was 95 %. There was no statistically significant difference between influent and filtered wastewater regarding the fraction  $<0.1\ \mu\text{m}$ , which both had a mean value of 105 mg/L. During the year of measurements, the size distribution of COD was fairly stable.

### 3.3. Models for removal of TSS and COD

A comparison between a linear model and an exponential model for prediction of TSS reduction ( $\text{TSS}_{\text{red}}$ ) towards the TSS in influent wastewater ( $\text{TSS}_{\text{in}}$ ), gave  $\text{TSS}_{\text{red}}\ (\text{mg/L}) = -36 \pm 6 + (0.80 \pm 0.03) \cdot \text{TSS}_{\text{in}}$  for the linear model (Fig. 3a) and  $k_1 = 0.74 \pm 0.04$ ,  $k_2 = 2.92 \pm 0.26$ , in the exponential model for determination of  $\text{TSS}_{\text{red}}\ (\%)$  in Eq. (1), (Fig. 3b). For the linear model, the correlation was similar regardless of TSS concentration in the influent within the range of 50–400 mg/L for  $\text{TSS}_{\text{in}}$ , while the accuracy for the exponential model was lower at higher influent TSS concentrations (Fig. 3c). It can also be noted how the standard deviations of the model impacted the predicted effluent TSS for the two models (Fig. 3c).

Linear models for COD removal ( $\text{COD}_{\text{red}}$ ; mg COD/L) based on  $\text{COD} > 1.6\ \mu\text{m}$ , coarse COD  $> 20\ \mu\text{m}$ , as well as total influent COD were compared for 27 samples during the period April 2021 to June 2021. The correlations were  $\text{COD}_{\text{red}} = -55 + 0.75 \times$ , ( $R^2 = 0.79$ ) for  $\text{COD} > 1.6\ \mu\text{m}$ ,  $\text{COD}_{\text{red}} = -18 + 0.79 \times$ , ( $R^2 = 0.77$ ) for coarse COD, and  $\text{COD}_{\text{red}} = -132 + 0.69 \times$ , ( $R^2 = 0.78$ ) for influent COD (Fig. S2). The linear model for  $\text{COD} > 1.6\ \mu\text{m}$  was used for calculation of the influent matrix in simulations of RBF and RBFF (Section 2.4). The resulting filtered wastewater COD in mg/L (Fig. S3) illustrates that the models based on coarse COD  $> 20\ \mu\text{m}$  and  $\text{COD} > 1.6\ \mu\text{m}$  rendered outputs with similar variability ( $304 \pm 37$  and  $305 \pm 34$  mg COD/L) compared to the measured values of  $304 \pm 36$  mg COD/L, while the outputs from the total influent COD model were less spread out ( $306 \pm 23$  mg COD/L).

### 3.4. Feasibility of fermentate addition to wastewater filtration

The mean TSS reduction with recirculation of fermented sludge to the influent wastewater was  $61 \pm 14\ \%$  (Table S4), which was slightly lower than the  $63 \pm 9\ \%$  without recirculation during the same period the previous year, December 2020 to May 2021. The variability of the TSS reduction was higher with recirculation. During the period with recirculation, the additional TSS load to the RBF filter caused peaks of TSS in the filtered wastewater. With the applied operational settings, the pumping of fermented sludge occurred during a few minutes every 1–2 h. The velocity of the filter belt increased during these periods, but did not cause overflow of wastewater. However, the recirculation of sludge to the filter caused lower fermentation yield during this period (Fig. S4). Due to the low fermentation yield and the measurement uncertainty for COD, no actual increase of soluble COD in the wastewater could be observed during the period with recirculation of fermented sludge (data not shown). Consequently, a design with a separate side-stream filter for separation of the fermented solids was adopted in the calculations of potential for increased soluble COD and VFAs, as well as in the simulated scenario RBFF.

### 3.5. Potential for increased soluble COD and VFA with addition of fermentate

The influent wastewater VFA concentration was variable, but displayed a noticeable seasonal variation (Fig. 4a). Curve fitting of the temperature dependency Eq. (2) rendered a value of  $\text{VFA}_{20} = 31 \pm 1$  mg HAC-eq/L with  $\theta = 1.12 \pm 0.02$  ( $R^2 = 0.54$ ) for VFA in influent wastewater. A sudden drop in the influent wastewater VFA could be noticed when the temperature was below  $12\ ^\circ\text{C}$ , and the measured values were lower compared to the fitted curve. The VFA increase in the wastewater owing to fermentate addition was calculated from the yield during one year of fermentation reactor operation without recirculation of fermented sludge. Temperature dependency was calculated (Eq. (2)) to  $\text{VFA}_{20} = 24 \pm 1$  mg HAC-eq/L with  $\theta = 1.08 \pm 0.01$  ( $R^2 = 0.68$ ; Fig. 4b). At low wastewater temperature of  $12\ ^\circ\text{C}$ , the influent VFA concentration for the filtered wastewater could potentially be doubled from  $\sim 12$  to  $\sim 25$  mg HAC-eq/L by adding fermented FPS. During summer, at  $20\ ^\circ\text{C}$ , an increase of  $\sim 24$  mg HAC-eq/L could be expected from the model, resulting in a total concentration of  $\sim 55$  mg HAC-eq/L (Fig. 4b). The average increase in the wastewater during the year (Table 2) was  $16 \pm 5$  mg HAC-eq/L, with a resulting total wastewater concentration of  $38 \pm 14$  mg HAC-eq/L. The soluble COD increase potential in the wastewater was  $39 \pm 9$  mg COD/L, of which  $31 \pm 9$  mg was VFA-COD (Table 2).

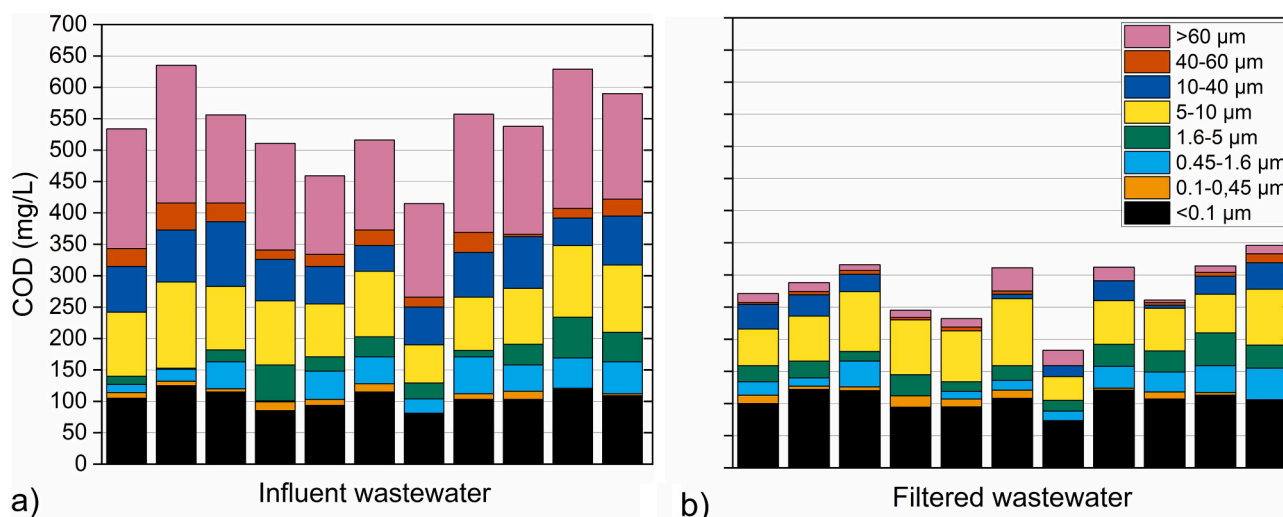
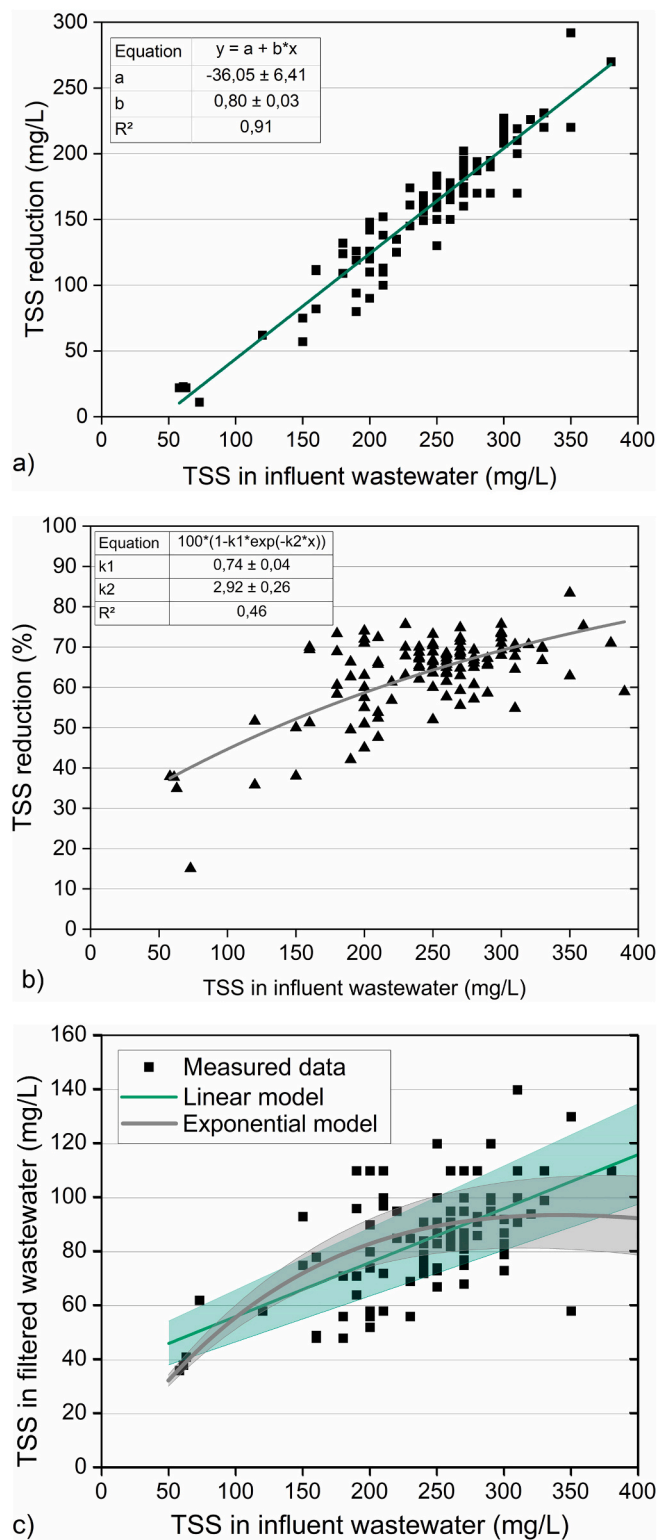
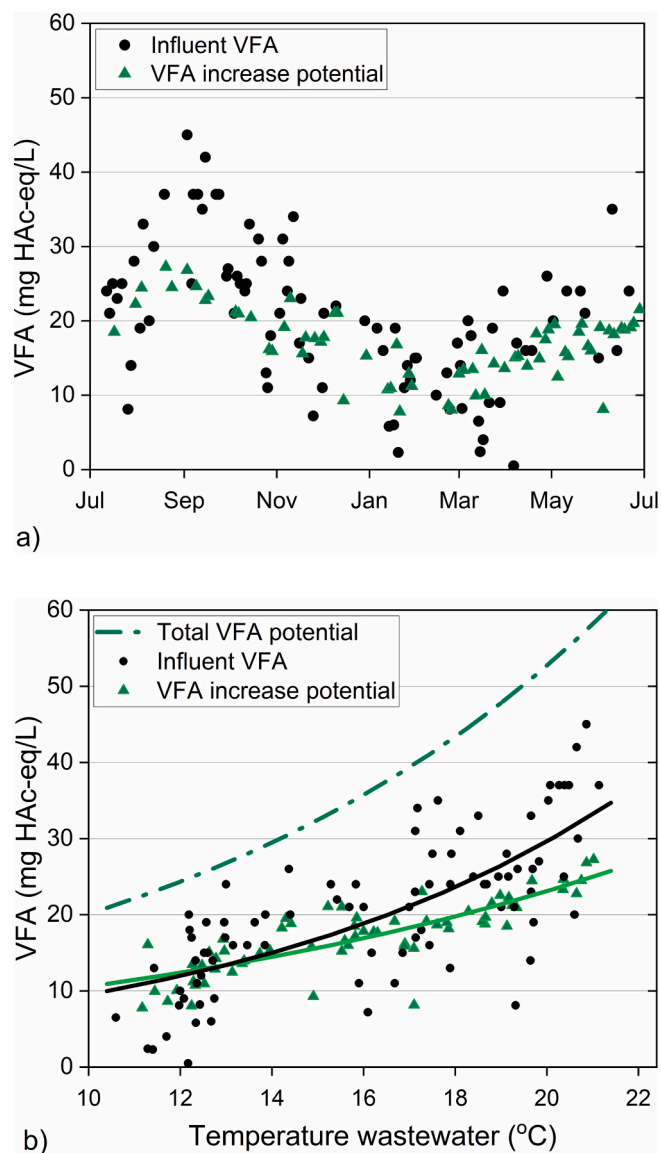


Fig. 2. COD characterisation in a) influent and b) filtered wastewater during one year of operation. Each bar represents one sample.



**Fig. 3.** Curve fitting of TSS reduction towards a) a linear model for TSS reduction versus influent TSS, b) an exponential model for percentual reduction versus influent TSS, and c) a comparison of the resulting TSS in filtered wastewater for both models including standard deviations for the fitted curves marked as areas, with the measured data.

The nutrient release in FPS fermentation at ambient temperature has been observed to remain rather constant during the year, which affects the COD to nutrient ratios in the fermentate (Ossiansson et al., 2023). The added ammonium from fermentate of  $1.9 \pm 0.5 \text{ NH}_4^+ \text{-N/L}$  (Table 2)



**Fig. 4.** a) Influent VFA concentration and VFA increase potential from fermentation of filter sludge at ambient temperature and 5 d retention time. b) VFA in influent wastewater and VFA increase, fitted to wastewater temperature, presented with their summarised total VFA potential.

**Table 2**

Increase and total concentrations of COD, VFA and nutrients in filtered wastewater owing to addition of fermentate of FPS at 5 d RT at ambient temperature during one year, presented as mean  $\pm$  standard deviation (n).

Parameter	Unit	Filtered wastewater	Increase in wastewater
COD <0.45 $\mu\text{m}$	mg COD/L	N.D.	$39 \pm 9$ (66)
Volatile fatty acids	mg COD/L	N.D.	$31 \pm 9$ (50)
Volatile fatty acids	mg HAC-eq/L	$20 \pm 10$ (85)	$17 \pm 5$ (66)
Ammonium nitrogen	mg $\text{NH}_4^+ \text{-N/L}$	$38 \pm 8$ (102)	$1.9 \pm 0.5$ (88)
Total nitrogen	mg N/L	$51 \pm 9$ (102)	$1.9 \pm 0.5$ (88)
Phosphate phosphorus	mg $\text{PO}_4^{3-} \text{-P/L}$	$3.8 \pm 0.6$ (29)	$0.7 \pm 0.2$ (88)
Total phosphorus	mg P/L	$5.4 \pm 1.0$ (102)	$0.7 \pm 0.2$ (88)

was, however, low compared to the filtered wastewater concentration of  $38 \pm 8 \text{ NH}_4^+ \text{-N/L}$  (Table 1). The ratios of COD/N and  $\text{COD}_{\text{filt}}/\text{NH}_4^+ \text{-N}$  could potentially be improved notably by fermentate addition: from  $5.8 \pm 0.9$  to  $6.4 \pm 1.0 \text{ g COD/g N}$ , and from  $2.8 \pm 0.8$  to  $4.5 \pm 0.5 \text{ g COD}_{\text{filt}}/\text{g NH}_4^+ \text{-N}$ . The potential increase in phosphate due to fermentate addition of  $0.7 \pm 0.2 \text{ mg P/L}$  constituted a higher fraction of the filtered wastewater concentration of  $5.4 \pm 1.0 \text{ mg P/L}$ , compared to the increase in nitrogen (Table 2). The mean ratios of  $\text{g COD/g P}$  before and after fermentate addition were  $53.8 \pm 7.3$  and  $54.2 \pm 7.1$ , with  $36.5 \pm 7.1$  and  $41.0 \pm 5.7 \text{ g COD}_{\text{filt}}/\text{g PO}_4^{3-} \text{-P}$ .

### 3.6. BNR volumes, effluent values and energy balances

#### 3.6.1. BNR volumes

The design volumes for BNR based on DWA standard procedure could be calculated for the standard BSM1 influent with settler and the RBFF influent, whereas the carbon source was insufficient in wastewater treated with RBF. It was required to apply a lower particle reduction in the filter or add external carbon source. Therefore, a decreased polymer dosing was assumed to increase the particulate COD in the wastewater by 12 % in the adjusted RBF influent compared to the RBFF alternative.

The BNR volume required to reach  $7 \text{ mg N/L}$  in the effluent was  $11,900 \text{ m}^3$  for the case with settler,  $10,600 \text{ m}^3$  for RBF, and  $9800 \text{ m}^3$  for RBFF. The corresponding nitrification volumes were  $7700$ ,  $6600$  and  $6300 \text{ m}^3$ . Thus, the total volumes with RBF and RBFF could be decreased by 11 and 18 %, respectively, compared to the alternative with settler. To reach the same nitrogen effluent value with settler as with the RBFF, of  $13.1 \text{ mg N/L}$ , a volume of  $12,900 \text{ m}^3$  would be required for the case TN 13.1.

#### 3.6.2. Effluent values based on simulations

Simulations with the default BSM1 plant setup and different influent matrices resulted in effluent values of  $15.6 \text{ mg N/L}$  for settler,  $16.7 \text{ mg/L}$  with RBF (with higher COD reduction) and  $14.0 \text{ mg/L}$  with RBFF

(Table S5). Simulations with the design volumes for the different pre-treatments were also conducted to quantify the effluent parameters, as well as the electricity demand and the sludge production which were needed for the energy balance. Although the alternatives were designed for the same effluent nitrogen of  $7 \text{ mg/L}$ , the simulated effluent values differed. The alternative with settler gave  $13.9 \text{ mg N/L}$ , whereas RBF gave higher effluent of  $14.4 \text{ mg N/L}$ , and RBFF  $13.1 \text{ mg N/L}$  (Table S5). A closer look at the effluent ammonium revealed that RBF treatment improved the conditions for nitrification compared to settler, decreasing the concentration from  $5.3$  to  $2.6 \text{ mg NH}_4^+ \text{-N/L}$  (RBF) and  $3.5 \text{ mg NH}_4^+ \text{-N/L}$  (RBFF). The denitrification, on the other hand, was impaired by less COD after RBF treatment, thus increasing the nitrate effluent concentration from  $8.6$  with settler to  $12.5 \text{ mg NO}_3^+ \text{-N/L}$ . With RBFF, the denitrification was enhanced, and the nitrate could be decreased to  $8.6 \text{ mg NO}_3^+ \text{-N/L}$ . The total COD and TSS effluent values were rather unaffected by the pre-treatments in this case.

#### 3.6.3. Energy balance

The COD balances for the different process alternatives are depicted in Fig. 5 including the flows of primary sludge and WAS that constitute the energy recovery potentials. Of the  $663 \text{ mg COD/L}$  into the WWTP, about  $48 \text{ mg COD/L}$  remained in the effluent. The case with RBF had the highest COD flow in the sludge to the anaerobic digestion,  $464 \text{ g COD/m}^3$  wastewater, and therefore the highest value for recovered COD in the biogas,  $233 \text{ g COD/m}^3$ . The settler and RBFF designs had similar values for biogas production of  $191$  and  $189 \text{ g COD/m}^3$  respectively.

The required electrical energy for aeration could be decreased by 18 % with RBFF compared to settler, and with 22 % compared to the case TN 13.1 with settler (Table 3), owing to smaller nitrification volumes. The smaller denitrification volumes required less mixing energy, but its effect on the total electricity demand was negligible. The energy input for pre-treatment was increased from  $0.004$  to  $0.02 \text{ kWh/m}^3$  with RBF. Nevertheless, the overall energy saving for pre-treatment and activated sludge treatment was  $0.04$  and  $0.05 \text{ kWh/m}^3$  for RBF and RBFF,

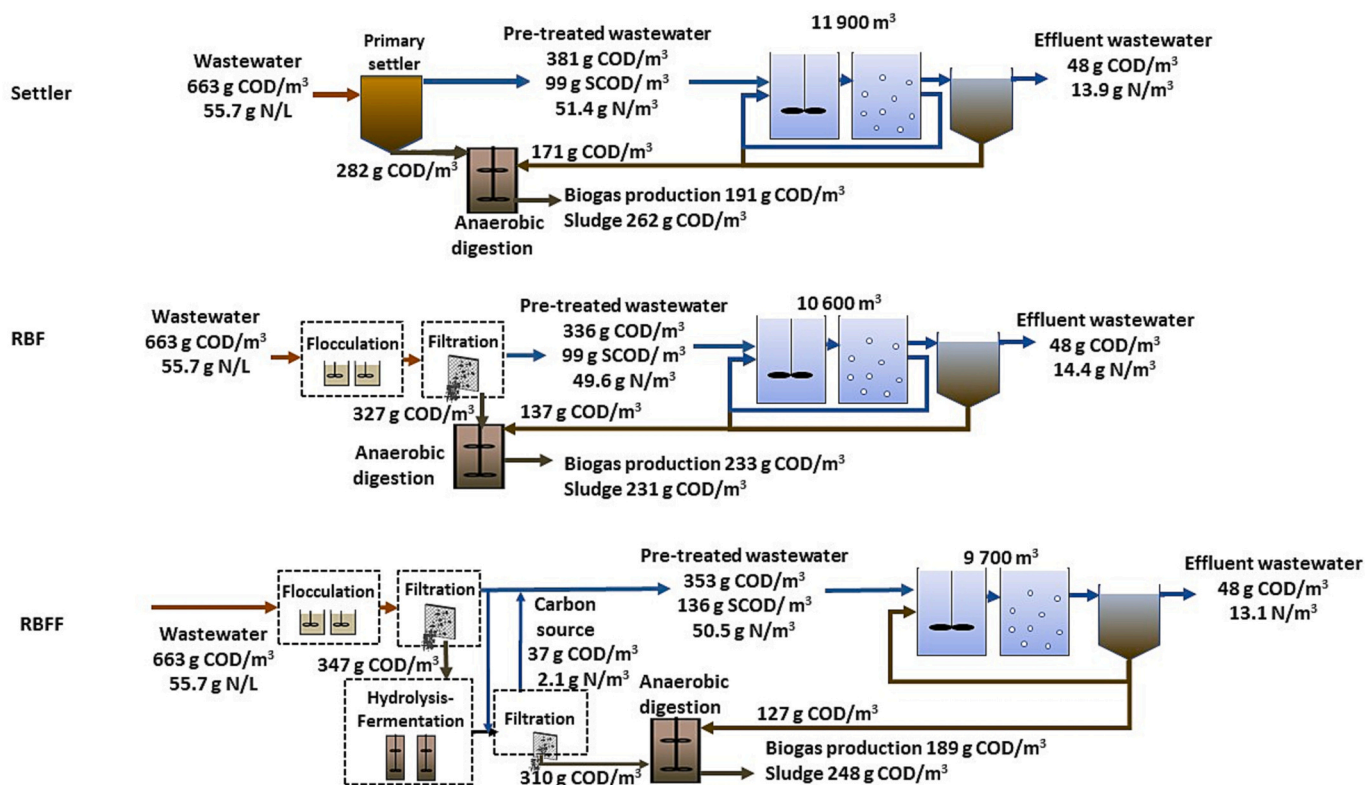


Fig. 5. Overview of COD flows for the three DWA design with BSM1 influent and pre-treatment with settler, RBF and RBFF. All COD flows are expressed as  $\text{g COD/m}^3$  of influent wastewater.



**Table 3**

Electrical energy requirement (kWh/m<sup>3</sup> wastewater) for the different WWTP designs.

	BSM1	DWA design			TN 13.1
	Settler	Settler	RBF	RBF	Settler
Pre-treatment	0.004	0.004	0.02	0.02	0.004
Denitrification (mixing)	0.01	0.03	0.03	0.02	0.03
Nitrification (aeration)	0.18	0.35	0.29	0.29	0.37
Recirculation flows (pumping)	0.02	0.02	0.02	0.02	0.02
Biological treatment	0.22	0.40	0.34	0.33	0.42
Total electrical energy input	0.22	0.40	0.36	0.35	0.43
Biogas energy production	0.72	0.67	0.82	0.66	0.67
Net energy production <sup>a</sup>	0.50	0.27	0.46	0.31	0.25

<sup>a</sup> Biogas production - total electrical energy input

respectively, corresponding to 11 and 13 % of the total electricity input.

The high biogas potential with RBF improved the net energy balance: 0.46 kWh/m<sup>3</sup> compared to 0.27 kWh/m<sup>3</sup> for settler and 0.31 kWh/m<sup>3</sup> for RBFF (Table 3). However, the RBF scenario resulted in higher effluent nitrogen (Table S5). The TN 13.1, which gave comparable nitrogen effluent as RBFF, but with settler, resulted a net energy balance of only 0.25 kWh/m<sup>3</sup>.

## 4. Discussion

### 4.1. The link between wastewater characteristics and filtration

Both the characteristics of the studied wastewater, and the removal efficiency in pre-filtration were representative to many other WWTPs. Coarse COD in the wastewater, filtered through >20 µm, constituted 56 ± 9 % of total COD, close to the 58 % based on characterisation of a wastewater in Norway (Razafimanantsoa et al., 2014). The COD concentrations in unfiltered, and 0.45 µm-filtered wastewater (Table 1) were similar compared to reported values for wastewater in Turkey (Tas et al., 2009), as well as the in Netherlands (Van Nieuwenhuijzen et al., 2001). The ratio of COD in filtered and unfiltered influent wastewater was 0.27, which is lower than 0.4, and thus meets the recommendation for filtration suitability (Rusten and Ødegaard, 2006). Furthermore, the average VFA-COD in the influent wastewater, calculated with the ratio of 1.7 g COD/g HAC-eq (Ossiansson et al., 2023) was 39 g COD/L, close to the typical value of 35 g COD/L found in Henze (1992) and the 20–65 mg COD/L measured in nine Korean WWTPs (Yun et al., 2013). The TSS removal of 64 % in this study is similar to the 66 % observed for chemically enhanced RBF filtration with comparable hydraulic load (Rusten et al., 2017). Moreover, the COD removal of 44 % in this study was similar to the 46 % for RBF filtration after addition of 2 mg polymer/m<sup>3</sup> (Franchi and Santoro, 2015) and 43 % reported for chemically enhanced sand filtration (Van Nieuwenhuijzen et al., 2001). The hydraulic load of 47 m<sup>3</sup>/ (m<sup>2</sup>, h) in this study can be compared to applied loads for chemically enhanced filtration of 25 m<sup>3</sup>/ (m<sup>2</sup>, h) (Rusten and Ødegaard, 2006) and 41–66 m<sup>3</sup>/ (m<sup>2</sup>, h) (Rusten et al., 2017).

The suitability of models for TSS reduction over RBF can possibly depend on the operating conditions. In this study, the linear model for TSS reduction in mg/L gave a satisfactory result and was suitable to use. Although the predictability of effluent TSS concentration had an error of ~30 mg/L with the linear model, it is still preferable compared to using the average percentual reduction for TSS effluent prediction. The data correlation to the exponential model for percentual reduction of TSS in the filter (Fig. 3b) was low (R<sup>2</sup> of 0.46), which indicates a rather poor correlation in this study. The same exponential model has been applied with a considerably higher R<sup>2</sup> value of 0.78 and 0.65 for 210 and 250 µm sieves respectively, with constant wastewater flow and without polymer dosing (Da Ros et al., 2020). The increase in TSS reduction at higher influent TSS reflects the impact of a filter mat filtration. With polymer addition, particle separation can be enhanced also at lower TSS concentrations, and the filter mat may consequently have less influence on

the TSS reduction. Another explanation can be the influent TSS concentration in this study, which is in the lower range compared to the data presented in Franchi and Santoro (2015) and da Ros et al. (2020).

Assessment of the linear model for prediction of the COD concentration in the wastewater after RBF showed a similar fit for all three types of input COD data: influent (total) COD and COD (>1.6 µm and >20 µm). However, the predictions based on COD (>1.6 µm and >20 µm) captured the variability in the wastewater content better than predictions based on influent COD. If a model for COD reduction based on influent COD is applied, it is recommended to use a safety factor for design purposes, but it is preferable to measure particulate COD to obtain a more accurate prediction of filter removal.

### 4.2. The effects of pre-treatments on subsequent BNR

The fermentation process was clearly seasonal (see Ossiansson et al., 2023 for details) resulting in a calculated VFA increase of 11–25 mg HAC-eq/L in the ambient wastewater temperature range of 11–22 °C (Fig. 4). This VFA increase appears to be comparable to fermentation conducted in a primary settler by means of elevated sludge blanket and sludge recirculation (in-line fermentation). VFA increases of 14–23 mg HAC-eq/L for in-line fermentation, and 16–36 mg HAC-eq/L for side-stream configuration were measured at 20 °C (Bouzas et al., 2007). In-line fermentation of SPS has increased the VFA content from 21 to 40 mg HAC-eq/L during summer in the same region (Hey et al., 2012), and from 20 to 50 mg HAC-eq/L during 1.5 year of operation (Tykesson et al., 2005), which is in the same range as the calculated VFA increase in our study. On the other hand, side-stream fermentation has the advantage of more control over the sludge retention time, as well as lower risk of process disturbance due to wastewater flow variations, and the possibility to adjust the addition of carbon source to the requirements in BNR.

The simulations confirm that the nitrogen removal is impaired by extensive carbon removal in filtration, but can be enhanced by FPS fermentation. Batch-tests with wastewater before and after filtration, compared with wastewater after addition of filtered fermentate has shown that the denitrification capacity is lower after filtration, and that fermentate raises both the denitrification rate, and the nitrate removal (Ossiansson et al., 2023).

The phosphate that is solubilised in the fermentation, would most likely have been solubilised in the anaerobic digestion if fermentation was not applied, and returned with the reject from dewatering of digested sludge. Unless phosphate recovery would have been applied for the reject stream, the phosphate which is added with the fermentate is not a real addition to the load. On the contrary, ammonium from fermentation can be a real addition to the load, depending on whether the anaerobic digestion is followed by separate treatment of reject water. The contribution from the reject water to the nitrogen load is normally 10–15 % (van Loosdrecht, 2008). The calculated addition of 1.9 ± 0.5 mg NH<sub>4</sub>-N/L would add ~4 % to the nitrogen load. Similar moderate additions of nitrogen from fermentation have been reported in other WWTPs (Banister et al., 1998; Bouzas et al., 2007) as well as no measurable increase in ammonium (Hey et al., 2012). If the ammonium from the fermentate would have been removed in this study, the potential decrease in activated sludge volume would have been 20 % for the RBFF case compared to the alternative with settler, instead of 18 %. Struvite precipitation of the fermentate has been tested for simultaneous removal of ammonium and phosphate, but the removal efficiency for nitrogen is only ~20 %, whereas 90 % of the phosphate can be captured in the struvite (Liu et al., 2020). The commonly applied designs for EBPR allows for VFA uptake and phosphate release prior to denitrification, hence, the VFAs would most likely benefit EBPR rather than denitrification. In a full-scale application, it would be possible to add wastewater with a high concentration of fermentate directly to anoxic zones/anoxic phase to prioritise nitrogen removal if necessary.

### 4.3. Energy balance with fermentation of primary sludge

The higher TSS reduction for RBF compared to the alternative with settler, resulted in higher total methane potential with RBF and a similar methane potential for the alternatives with settler and RBFF. A previous comparison between RBF and settler, both coupled with sludge fermentation, gave higher TSS removal, and higher production of both carbon source and methane for settler than for RBF (Bahreini et al., 2021). However, the TSS-removal was set to a lower value of 45 % for RBF, and 70 % for settler which is as high as the expected reduction with chemically enhanced primary settling (Ho et al., 2017). The operation of an RBF has a profound effect on the TSS-removal efficiency, which can be higher than settler if operated with a thick filter mat, and lower than settler if operated at higher hydraulic load without filter mat (Behera et al., 2018). The methane potential from FPS has been measured to be lower than SPS (Bahreini et al., 2020), similar to SPS (Odirile et al., 2021) or higher than SPS (Paulsrud et al., 2014). In this study, the potential of FPS was set to a 10 % higher value than SPS, since tests indicated a higher potential with the applied pilot setup (Blom, 2022). An increase in methane potential of primary sludge after acidogenic fermentation has been shown (Levine et al., 1991), as well as similar methane potential even after withdrawal of fermentate (Jönsson et al., 2009). On the other hand, a comparison between raw and fermented sludge gave 6 and 18 % lower methane potential after 4 d fermentation for FPS and SPS, respectively (Bahreini et al., 2020). Since methane potential tests showed ~15 % lower potential for fermented FPS than raw FPS (Blom, 2022), and since 16 % of the VS was removed with the fermentate, the resulting methane potential in this study was 27 % lower for each kg VS removed in filtration in the RBFF scenario than in the RBF scenario. In conclusion, the efficiency of the pre-treatment can be increased by chemical addition, both for settlers and for filtration, and the case-studies should be interpreted from their set conditions. It is clear that primary sludge fermentation is likely to reduce the methane potential, unless it is balanced by a higher TSS removal in the primary treatment.

The simulations of activated sludge in this study showed that a pre-treatment with filtration and addition of fermentate increases the volumetric capacity, and decreases the electricity demand of a subsequent activated sludge process by 11 % for RBF and 13 % for RBFF. A similar saving (for plant-wide energy input) of 11 % with RBF has been shown in simulations (Pasini et al., 2021). Life-cycle analysis of a process with chemically enhanced micro-sieving (5–7 g polymer/m<sup>3</sup>), followed by BNR in biofilter showed that the carbon footprint and energy requirement for chemical production and consumption was minor for polymer addition to primary filtration compared to that of external carbon source (Remy et al., 2014).

### 4.4. Full-scale application

The operation with addition of fermented sludge prior to filtration could verify that this configuration is feasible, and that the negative effect on the total TSS reduction was minor. For future applications, it is, however, recommended to recirculate the fermented sludge to a separate filter instead of back to the main stream filter. The separated fermented FPS particles can then be directed to anaerobic digestion, rather than to fermentation with extended sludge retention time. In a full-scale application, the pumping of fermented sludge could be evened out to avoid sudden increase of TSS load. High velocity of the RBF will decrease efficiency as the newly exposed filter area without a filter mat increase. Therefore, operating the RBF with a more even TSS concentration in the influent will benefit TSS reduction.

Addition of fermentate should be applied only if it is beneficial for the effluent values, and for the energy balance. For a wastewater with a higher content of soluble COD, carbon source addition may not be needed to reach the effluent requirement for nitrogen. Instead, it can be applied for EBPR and/or to achieve a very low effluent value for total

nitrogen. This exemplifies the importance of applying a pre-treatment that is appropriate for the effluent requirements and influent wastewater characteristics, in order to design a compact and energy-efficient BNR.

## 5. Conclusions

- Pre-treatment with chemically enhanced RBF gave TSS reduction of  $64 \pm 10$  % with hydraulic load of  $47 \pm 11$  m<sup>3</sup>/(m<sup>2</sup>, h) and polymer dose of  $3.2 \pm 1.0$  g/m<sup>3</sup>.
- Particles >10 µm were removed effectively in the filtration.
- A linear model for TSS removal (mg/L) was preferable for prediction of TSS removal in RBF filtration, compared to an exponential model for TSS reduction (%).
- Addition of fermentate to wastewater, and particle separation through RBF filtration was a feasible option to transfer the carbon source to the wastewater prior to BNR. Since recirculation of sludge to the fermentation process caused decreased VFA yield, we recommend to use separate side-stream filtration to capture the particles from the fermented sludge, and to use this sludge for biogas production.
- The required design volumes for activated sludge in this study could be reduced by 11 % with RBF and 18 % with RBFF as pre-treatments compared to settler.
- RBFF enhanced nitrogen removal, and gave similar biogas production compared to primary settler without sludge fermentation. RBF could render the most favourable energy balance, but caused increased effluent nitrogen concentrations compared to the alternatives with settler and RBFF.

## CRediT authorship contribution statement

**Elin Ossiansson:** Conceptualization, Methodology, Resources, Visualization, Formal analysis, Investigation, Funding acquisition, Writing – original draft, Writing – review & editing, Project administration. **Simon Bengtsson:** Conceptualization, Methodology, Writing – review & editing, Supervision. **Frank Persson:** Methodology, Funding acquisition, Writing – review & editing, Supervision. **Michael Cimbritz:** Methodology, Writing – review & editing, Supervision. **David J.I. Gustavsson:** Conceptualization, Methodology, Funding acquisition, Project administration, Writing – review & editing, Supervision.

## Declaration of competing interest

The authors declare the following financial interests/personal relationships which may be considered as potential competing interests: David Gustavsson, VA SYD reports financial support was provided by Swedish Environmental Protection Agency. David Gustavsson reports financial support was provided by Sweden Water Research. David Gustavsson reports financial support was provided by The Swedish Water & Wastewater Association. Frank Persson reports financial support was provided by Foundation for J Gust Richerts minne.

## Data availability

Data will be made available on request.

## Acknowledgements

The pilot plant investment was partially funded by the Swedish Environmental Agency within the program City Innovations (NV-02084-18). The operation of the pilot plant was partially funded by VA SYD, Sweden Water Research, the foundation for J. Gust Richerts minne (2021-00753), and by the Swedish Water and Wastewater Association (19-112). Furthermore, the authors would like to acknowledge the laboratory (VA SYD) for their analyses, and the operational personnel at

Källby WWTP (VA SYD), as well as the master thesis students Sara Tebini, Sanna Sahlin and Fanny Blom. We would also like to thank Dr. Fabio Polesel (DHI) for assistance with the WEST model, and Salsnes Filter for technical support regarding the RBF. The authors would also like to thank Prof. Gustaf Olsson for his contribution in the course Water Energy Nexus.

## Appendix A. Supplementary data

Supplementary data to this article can be found online at <https://doi.org/10.1016/j.scitotenv.2023.166483>.

## References

- Amerlinck, Y., 2015. Model Refinements in View of Wastewater Treatment Plant Optimization: Improving the Balance in Sub-Model Detail. PhD Thesis.. Ghent University.
- Andreasen, K., Petersen, G., Thomsen, H., Strube, R., 1997. Reduction of nutrient emission by sludge hydrolysis. *Water Sci. Technol.* 35, 79–85. [https://doi.org/10.1016/S0273-1223\(97\)00215-1](https://doi.org/10.1016/S0273-1223(97)00215-1).
- Arnell, M., Rahmberg, M., Oliveira, F., Jeppsson, U., 2017. Multi-objective performance assessment of wastewater treatment plants combining plant-wide process models and life cycle assessment. *J. Water Clim. Chang.* 8, 715–729. <https://doi.org/10.2166/wcc.2017.179>.
- Bahreini, G., Elbeshbishy, E., Jimenez, J., Santoro, D., Nakhla, G., 2020. Integrated fermentation and anaerobic digestion of primary sludges for simultaneous resource and energy recovery: impact of volatile fatty acids recovery. *Waste Manag.* 118, 341–349. <https://doi.org/10.1016/j.wasman.2020.08.051>.
- Bahreini, G., Elbahravi, M., Elbeshbishy, E., Santoro, D., Nakhla, G., 2021. Biological nutrient removal enhancement using fermented primary and rotating belt filter biosolids. *Sci. Total Environ.* 796, 148947. <https://doi.org/10.1016/j.scitotenv.2021.148947>.
- Banister, S.S., Pitman, A.R., Pretorius, W.A., 1998. Quantification of N and P Release in Different Sludges 24, 337–342.
- Behera, C.R., Santoro, D., Gernaey, K.V., Sin, G., 2018. Organic carbon recovery modeling for a rotating belt filter and its impact assessment on a plant-wide scale. *Chem. Eng. J.* 334, 1965–1976. <https://doi.org/10.1016/j.cej.2017.11.091>.
- Blom, F., 2022. How the Choice of Primary Treatment Affects the Biogas Potential of Primary Sludge. Lund University, Master Thesis.
- Boiocchi, R., Behera, C.R., Sherratt, A., DeGroot, C.T., Gernaey, K.V., Sin, G., Santoro, D., 2020. Dynamic model validation and advanced polymer control for rotating belt filtration as primary treatment of domestic wastewaters. *Chem. Eng. Sci.* 217, 115510. <https://doi.org/10.1016/j.ces.2020.115510>.
- Bouzas, A., Ribes, J., Ferrer, J., Seco, A., 2007. Fermentation and elutriation of primary sludge: effect of SRT on process performance. *Water Res.* 41, 747–756. <https://doi.org/10.1016/j.watres.2006.11.034>.
- Caliskaner, O., Tchobanoglous, G., Imani, L., Davis, B., 2021. Performance evaluation of first full-scale primary filtration using a fine pore cloth media disk filter. *Water Environ. Res.* 93, 94–111. <https://doi.org/10.1002/wer.1358>.
- Canziani, R., Pollice, A., Ragazzi, M., 1996. Design considerations on primary sludge hydrolysis under psychrophilic conditions. *Environ. Technol. (United Kingdom)* 17, 747–754. <https://doi.org/10.1080/09593331708616441>.
- Christensen, M.L., Jakobsen, A.H., Hansen, C.S.K., Skovbjerg, M., Andersen, R.B.M., Jensen, M.D., Sundmark, K., 2022. Pilot-scale hydrolysis of primary sludge for production of easily degradable carbon to treat biological wastewater or produce biogas. *Sci. Total Environ.* 846, 157532. <https://doi.org/10.1016/j.scitotenv.2022.157532>.
- Da Ros, C., Conca, V., Eusebi, A.L., Frison, N., Fatone, F., 2020. Sieving of municipal wastewater and recovery of bio-based volatile fatty acids at pilot scale. *Water Res.* 174, 115633. <https://doi.org/10.1016/j.watres.2020.115633>.
- DWA, 2016. DWA Set of Rules. Standard DWA-A 131E. Dimensioning of Single-Stage Activated Sludge Plants. German Association for Water.
- Franchi, A., Santoro, D., 2015. Current status of the rotating belt filtration (RBF) technology for municipal wastewater treatment. *Water Pract. Technol.* 10, 319–327. <https://doi.org/10.2166/wpt.2015.038>.
- Gernaey, K.V., Alex, J., Copp, J., 2009. Primary Clarifier Model for BSM2 Application [WWW Document]. PubPub. URL <https://assets.pubpub.org/ujzz1t74/01603272493900.pdf> (accessed 11.29.22).
- Gernaey, K.V., Jeppsson, U., Vanrolleghem, P.A., Copp, J.B., 2015. Benchmarking of Control Strategies for Wastewater Treatment Plants, Benchmarking of Control Strategies for Wastewater Treatment Plants. IWA Publishing. <https://doi.org/10.2166/9781780401171>.
- Gustavsson, D.J.I., Tumlin, S., 2013. Carbon footprints of Scandinavian wastewater treatment plants. *Water Sci. Technol.* 68, 887–893. <https://doi.org/10.2166/wst.2013.318>.
- Henze, M., 1992. Characterization of wastewater for modelling of activated sludge processes. *Water Sci. Technol.* 25, 1–15. <https://doi.org/10.2166/wst.1992.0110>.
- Hey, T., Jönsson, K., La Cour Jansen, J., 2012. Full-scale in-line hydrolysis and simulation for potential energy and resource savings in activated sludge - a case study. *Environ. Technol.* 33, 1819–1825. <https://doi.org/10.1080/09593330.2011.650217>.
- Ho, D., Scott, Z., Sarathy, S., Santoro, D., 2017. Enhanced primary treatment. *Innovative Wastewater Treatment & Resource Recovery Technologies Impacts on Energy, Economy and Environment*. 155–176.
- Ibrahim, V., Hey, T., Jönsson, K., 2014. Determining short chain fatty acids in sewage sludge hydrolysate: a comparison of three analytical methods and investigation of sample storage effects. *J. Environ. Sci.* 26, 926–933. [https://doi.org/10.1016/S1001-0742\(13\)60516-1](https://doi.org/10.1016/S1001-0742(13)60516-1).
- Jeppsson, U., 2009. Benchmark simulation models [WWW document] BSM1. <https://github.com/wwtmodels/Benchmark-Simulation-Models> (accessed 1.11.23).
- Jönsson, K., Hey, T., Norlander, H., Nyberg, U., 2009. Impact on gas potential of primary sludge hydrolysis for internal carbon source production. In: 2nd IWA Spec. Conf. Nutr. Manag. Wastewater Treat. Process.
- Khan, F.A., Chowdhury, P., Giaccherini, F., Straatman, A.G., Santoro, D., 2021. Detailed modeling of solids separation by microsieving in a rotating belt filter: explicit effect of particle size, mesh size, and polymer dose. *Sep. Purif. Technol.* 269. <https://doi.org/10.1016/j.seppur.2021.118777>.
- Levine, A.D., Tchobanoglous, G., Asano, T., 1991. Size distributions of particulate contaminants in wastewater and their impact on treatability. *Water Res.* 25, 911–922. [https://doi.org/10.1016/0043-1354\(91\)90138-G](https://doi.org/10.1016/0043-1354(91)90138-G).
- Liu, Q., Li, Y., Yang, F., Liu, X., Wang, D., Xu, Q., Zhang, Y., Yang, Q., 2021. Understanding the mechanism of how anaerobic fermentation deteriorates sludge dewaterability. *Chem. Eng. J.* 404, 127026. <https://doi.org/10.1016/j.cej.2020.127026>.
- Liu, W., Yang, H., Ye, J., Luo, J., Li, Y.Y., Liu, J., 2020. Short-chain fatty acids recovery from sewage sludge via acidogenic fermentation as a carbon source for denitrification: a review. *Bioresour. Technol.* 311, 123446. <https://doi.org/10.1016/j.biortech.2020.123446>.
- Longo, S., d'Antoni, B.M., Bongards, M., Chaparro, A., Cronrath, A., Fatone, F., Lema, J. M., Mauricio-Iglesias, M., Soares, A., Hospido, A., 2016. Monitoring and diagnosis of energy consumption in wastewater treatment plants. A state of the art and proposals for improvement. *Appl. Energy* 179, 1251–1268. <https://doi.org/10.1016/j.apenergy.2016.07.043>.
- Odirile, P.T., Marumolao, P.M., Manali, A., Gikas, P., 2021. Anaerobic digestion for biogas production from municipal sewage sludge: a comparative study between fine mesh sieved primary sludge and sedimented primary sludge. *Water (Switzerland)* 13. <https://doi.org/10.3390/w13243532>.
- Ossiansson, E., Persson, F., Bengtsson, S., Cimbritz, M., Gustavsson, D.J.I., 2023. Seasonal variations in acidogenic fermentation of filter primary sludge. *Water Res.* 242, 120181. <https://doi.org/10.1016/j.watres.2023.120181>.
- Pasini, F., Garrido-Baserba, M., Ahmed, A., Nakhla, G., Santoro, D., Rosso, D., 2021. Oxygen transfer and plant-wide energy assessment of primary screening in WRRFs. *Water Environ. Res.* 93, 677–692. <https://doi.org/10.1002/wer.1349>.
- Patziger, M., Kiss, K., 2015. Analysis of suspended solids transport processes in primary settling tanks. *Water Sci. Technol.* 72, 1–9. <https://doi.org/10.2166/wst.2015.168>.
- Paulsrud, B., Rusten, B., Aas, B., 2014. Increasing the sludge energy potential of wastewater treatment plants by introducing fine mesh sieves for primary treatment. *Water Sci. Technol.* <https://doi.org/10.2166/wst.2013.737>.
- Razafimanantsoa, V.A., Ydstebø, L., Bilstad, T., Sahu, A.K., Rusten, B., 2014. Effect of selective organic fractions on denitrification rates using Salsnes Filter as primary treatment. *Water Sci. Technol.* 69, 1942–1948. <https://doi.org/10.2166/wst.2014.110>.
- Razafimanantsoa, V.A., Adyasari, D., Sahu, A.K., Rusten, B., Bilstad, T., Ydstebø, L., 2019. Pilot-scale study to investigate the impact of rotating belt filter upstream of a MBR for nitrogen removal. *Water Sci. Technol.* 79, 458–465. <https://doi.org/10.2166/wst.2019.069>.
- Remy, C., Boulestreau, M., Lesjean, B., 2014. Proof of concept for a new energy-positive wastewater treatment scheme. *Water Sci. Technol.* 70, 1709–1716. <https://doi.org/10.2166/wst.2014.436>.
- Rieger, L., Gillot, S., Langergraber, G., Ohtsuki, T., Shaw, A., Takács, I., Winkler, S., 2013. Guidelines for Using Activated Sludge Models. IWA Publishing, Water Intelligence Online. <https://doi.org/10.2166/9781780401164>.
- Rusten, B., Ødegaard, H., 2006. Evaluation and testing of fine mesh sieve technologies for primary treatment of municipal wastewater. *Water Sci. Technol.* 54, 31–38. <https://doi.org/10.2166/wst.2006.710>.
- Rusten, B., Razafimanantsoa, V.A., Andriamiarinjaka, M.A., Otis, C.L., Sahu, A.K., Bilstad, T., 2016. Impact of fine mesh sieve primary treatment on nitrogen removal in moving bed biofilm reactors. *Water Sci. Technol.* 73, 337–344. <https://doi.org/10.2166/wst.2015.498>.
- Rusten, B., Rathnaweera, S.S., Rismyr, E., Sahu, A.K., Ntiako, J., 2017. Rotating belt sieves for primary treatment, chemically enhanced primary treatment and secondary solids separation. *Water Sci. Technol.* 75, 2598–2606. <https://doi.org/10.2166/wst.2017.145>.
- Salsnes Filter, 2016. Eco-Efficient Solids Separation Benchmarking Water Solutions.
- Siegrist, H., Salzgeber, D., Eugster, J., Joss, A., 2008. Anammox brings WWTP closer to energy autarky due to increased biogas production and reduced aeration energy for N-removal. *Water Sci. Technol.* 57, 383–388. <https://doi.org/10.2166/wst.2008.048>.
- Tas, D.O., Karahan, Ö., Insel, G., Övez, S., Orhon, D., Spanjers, H., 2009. Biodegradability and denitrification potential of Setttable chemical oxygen demand in domestic wastewater. *Water Environ. Res.* 81, 715–727. <https://doi.org/10.2175/106143009x425942>.
- Tykesson, E., Jönsson, L.E., la Cour Jansen, J., 2005. Experience from 10 years of full-scale operation with enhanced biological phosphorus removal at Öresundsverket. *Water Sci. Technol.* 52, 151–159. <https://doi.org/10.2166/wst.2005.0451>.

- Väänänen, J., Cimbritz, M., La Cour Jansen, J., 2016. Microsieving in primary treatment: effect of chemical dosing. *Water Sci. Technol.* 74, 438–447. <https://doi.org/10.2166/wst.2016.223>.
- van Loosdrecht, M.C.M., 2008. Innovative Nitrogen Removal. In: Henze, M., van Loosdrecht, M.C.M., Ekama, G.A., Brdjanovic, D. (Eds.), *Biological Wastewater Treatment: Principles. IWA Publishing, Modelling and Design*, pp. 139–154.
- Van Nieuwenhuijzen, A.F., Van Der Graaf, J.H.J.M., Mels, A.R., 2001. Direct influent filtration as a pretreatment step for more sustainable wastewater treatment systems. *Water Sci. Technol.* 43, 91–98. <https://doi.org/10.2166/wst.2001.0671>.
- van Nieuwenhuijzen, A.F., van der Graaf, J.H.J.M., Kampschreur, M.J., Mels, A.R., 2004. Particle related fractionation and characterisation of municipal wastewater. *Water Sci. Technol.* 50, 125–132. <https://doi.org/10.2166/wst.2004.0704>.
- Yun, Z., Yun, G.H., Lee, H.S., Yoo, T.U., 2013. The variation of volatile fatty acid compositions in sewer length, and its effect on the process design of biological nutrient removal. *Water Sci. Technol.* 67, 2753–2760. <https://doi.org/10.2166/wst.2013.192>.